Selective inhibition of PKCβ2 preserves cardiac function after myocardial infarction and is associated with improved angiogenesis of ischemic myocardium in diabetic rats

FABIN WANG*, DONG HUANG*, WEI ZHU, SHUAI LI, MEILING YAN, MENG WEI and JINGBO LI

Division of Cardiology, Shanghai Sixth Hospital, Shanghai Jiao Tong University School of Medicine, State Key Discipline Division, Shanghai 200233, P.R. China

Received May 31, 2013; Accepted August 21, 2013

DOI: 10.3892/ijmm.2013.1477

Abstract. Activation of PKCβ2 induced by hyperglycemia contributes to impaired angiogenesis in endothelial cells. The purpose of the present study was to investigate whether PKCβ2 inhibition can attenuate the hyperglycemia-induced impaired angiogenesis of myocardium to improve cardiac function following myocardial infarction (MI) in diabetes. *In vitro*, human umbilical vein endothelial cells (HUVECs) were cultured in low glucose (L-G) (5.6 mmol/l) or high glucose (H-G) (33.3 mmol/l) medium in the presence or absence of LY333531 (LY333) (10 nmol/l), a selective PKCβ2 inhibitor. *In vivo*, with the use of an MI diabetic rat model, animals were randomized to receive LY333 (10 mg/kg/day) orally for 4 weeks after MI, or no treatment whatsoever. Treatment of HUVECs with LY333 prevented the H-G-induced decrease of tube formation, migration and proliferation. Furthermore, exposure of HUVECs to H-G activated PKCβ2 and decreased levels of phospho-Akt (p-Akt) and phospho-endothelial nitric oxide synthase (p-eNOS) expression, which was also prevented by LY333. Compared with MI rats without therapy, LY333-treated MI rats showed an increase in left ventricular ejection fraction (LVEF) and fractional shortening (FS), but a reduction in infarct size. Furthermore, treatment of rats with LY333 not only significantly increased the capillary density of ischemic myocardium, but also significantly elevated the levels of p-Akt and p-eNOS expression. We also observed a significant increase of VEGF expression in myocardium measured by immunostaining in MI and LY333 groups compared to sham group. Anti-CD31 immunostaining revealed that MI rats treated with LY333 exhibited increased density of capillaries compared with sham group rats. However, treatment of rats with LY333 did not result in significant increases in vascular endothelial growth factor (VEGF) expression at both the mRNA and protein levels in myocardium, and in the plasma level of VEGF compared with MI rats without therapy. Overall, these results suggest that inhibition of PKCβ2 may be a novel therapeutic approach for preserving cardiac function after MI, in part by improving impaired angiogenesis of myocardium in diabetes.

Correspondence to: Professor Jingbo Li, Division of Cardiology, Shanghai Sixth Hospital, Shanghai Jiao Tong University School of Medicine, State Key Discipline Division, 600 Yishan Road, Shanghai 200233, P.R. China
E-mail: lijb_2006@sina.cn

*Contributed equally

Key words: PKCβ2, myocardial infarction, cardiac function, angiogenesis, diabetes

Introduction

Myocardial infarction (MI) is one of the most severe coronary artery diseases. The effective formation of coronary collateral arteries post-MI plays an important role in the recovery of cardiac function. However, patients with diabetes mellitus exhibit less collateral formation of coronary artery after MI (1) and are at high risk of heart failure following MI compared to non-diabetic patients (2-4). Samuel *et al* (5) have recently shown that administration of adenoviral vascular endothelial growth factor (VEGF) increases angiogenesis and reduces ventricular remodeling in the infarcted diabetic myocardium, suggesting that the impaired angiogenesis of diabetic myocardium is associated with a decreased VEGF expression in animal models of MI.

PKCβ2 is a classical isoform of the PKC family of serine/threonine kinases and is preferentially activated in the aorta and heart under diabetic conditions. PKCβ2 activation decreases the PI3-kinase/Akt-dependent endothelial nitric oxide synthase (eNOS) activation in response to VEGF or insulin stimulation (6,7). Recent studies have shown that PKCβ2 is activated following MI, and LY333531 (LY333), an oral selective inhibitor of PKCβ2, attenuates MI-induced heart failure in non-diabetic rats, which is associated with reduction of fibrosis and pro-inflammatory responses (8,9). However, there is still a lack of data on whether inhibition of PKCβ2 increases angiogenesis of the myocardium, which is associated with upregulation of the Akt/eNOS pathway in diabetes and whether the effect can preserve cardiac function after MI.

Therefore, we used a diabetic rat model with MI and a human umbilical vein endothelial cells (HUVECs) culture to investigate the *in vivo* and *in vitro* effects and mechanisms by which LY333 may prevent cardiac dysfunction after MI with a focus on PKCβ2-dependent signaling.

Materials and methods

Cell culture and treatment. HUVECs were obtained from the American Type Culture Collection (ATCC, Manassas, VA, USA). Cells were cultured in Dulbecco's modified Eagle's medium (DMEM) containing 10% BSA (Gibco-Invitrogen Inc., Carlsbad, CA, USA), 0.05 mg/ml endothelial growth factor (Sigma, St. Louis, MO, USA), 0.1 mg/ml heparin, 100 U/ml penicillin and 100 mg/ml streptomycin at 37˚C under 5% CO_2. The cells used in subsequent experiments were from passages 2-4. HUVECs were randomly divided into 3 groups: low glucose group (L-G, 5.6 mmol/l), high glucose group (H-G, 33.3 mmol/l), and high glucose + LY333531 (H-G + LY333, 10 nmol/l).

Cell tube formation assay. Tube formation assay in HUVECs was performed by a Matrigel assay as previously described (10). Briefly, 50 μl Matrigel were transferred to a 96-well plate and were allowed to polymerize at 37˚C, 5% CO_2 for 1 h. HUVECs were seeded at $1x10^4$/well and cultured in the presence or absence of different types of reagents, for 18 h. Tube formation was observed using a microscope and images were captured with a computer system. Images were subjected to image processing using the Image-Pro Plus software (Media Cybernetics, Inc., Rockville, MD, USA) to calculate the degree of tube formation by measuring the length of tubes in three random low-power (x40) fields from each well. The L-G group was defined as the control group (100% tube formation). Tube formation in the other groups was expressed in relation to the control.

Cell migration assay. A wound healing assay was performed as previously described (11). In brief, wounds were produced by scraping a cell layer with a 200 μl pipette tip and the boundary of the wound was marked. Phosphate-buffered saline was used to rinse the cells twice, in order to remove cellular debris and to dislodge cells. The cells were cultured in the presence of different reagents for 24 h. Wounds were observed with a microscope at x40. The ability of cell migration was calculated by the formula: $100\%-(width_{24\,h}/width_{0\,h})$ x100% (12).

Cell proliferation assay. Cell proliferation was determined using the 3-(4,5-dimethylthiazol-2-yl)-2,5-diphenyltetrazolium bromide (MTT) assay (Sigma). HUVECs were seeded in 96-well plates at a density of $5x10^3$/well according to the grouping. After 24 h, the curve of cell proliferation was obtained at 490 nm with a 96-well plate reader.

Ethics statement. The animal research study protocol was in compliance with 'The Guide for the Care of Use of Laboratory Animals' published by the National Institute of Health (NIH publication no. 85-23, revised 1996). The animal experiments were approved by the Animal Care Committee of the Shanghai Sixth Hospital, Shanghai Jiao Tong University School of Medicine. The rats were housed for 2 weeks as an acclimatization period prior to the experiment.

Animal protocol. Forty male adult Sprague-Dawley (SD) rats, weighing 250-300 g (Experimental Animal Center, Chinese Academy of Sciences, Shanghai, China) were induced to a diabetic state by intraperitoneal injection of streptozotocin (STZ, 50 mg/kg in sodium citrate buffer; Sigma) (13). One week after STZ injection, blood glucose levels were measured, and animals with glucose levels ≤300 mg/dl were excluded from the study.

A total of 35 diabetic rats were anesthetized by intraperitoneal injection of pentobarbital sodium (60 mg/kg) and animals were ventilated using an animal respirator DW-200 (Alcott Biotech, Shanghai, China) with room air after endotracheal intubation. The electrocardiogram (ECG) lead II was continuously monitored during the experiment. Heart exposure was performed by a thoracotomy at the left fourth intercostal space. The left anterior descending (LAD) coronary artery was ligated using a 6-0 prolene suture, 1-2 mm below the tip of the left atrial appendage. LAD ligation was confirmed by the elevation of the ST segment. All the surviving rats were randomly assigned into i) MI group (n=14), where rats did not receive any therapy; ii) LY333 group (n=14), where MI rats received oral LY333 (10 mg/kg/day, by gastric gavage) for 4 weeks starting 3 days after LAD ligation. Another 10 rats, as a control group, underwent thoracotomy and incision of the pericardial sac, but not LAD ligation. Four weeks after LAD ligation, all the surviving rats were sacrificed.

Echocardiography and hemodynamics. Before rats were sacrificed, transthoracic echocardiography was performed 4 weeks after MI using a standard ultrasound system equipped with a 15-MHz probe and an Acuson Sequoia 512 (Siemens, Erlangen, Germany). Left ventricular end-systolic (LVESd) and left ventricular end-diastolic diameters (LVEDd) were measured. In addition, left ventricular ejection fraction (LVEF) and fractional shortening (FS) were calculated, as previously described (14). Five consecutive cardiac cycles were averaged for all the analyses. Thereafter, hemodynamic measurements were also performed by cardiac catheterization. The right carotid artery was cannulated with a pre-heparinized fine PE tube connected to a fluid-filled pressure transducer (MPA-CFS; Alcott Biotech). Left ventricular end-diastolic pressure (LVEDP), heart rate (HR) and the maximal rates of positive and negative pressure change ($\pm dP/dT_{max}$) were recorded.

Infarct size. Masson's trichrome-stained slides were used to determine the infarct size. Infarct size was calculated as the ratio of the average scar circumferences of the endocardium and epicardium to the average left ventricular circumferences of the endocardium and the epicardium, as described in a previous study (8).

Real-time RT polymerase chain reaction. Total RNA was extracted from 100 mg of LV-free wall using TRIzol reagent (Gibco-Invitrogen). Two micrograms of RNA were processed directly to cDNA with the moloney murine leukemia virus (M-MLV) reverse transcriptase (Promega, Madison, WI,

USA). The primers for rat $VEGF_{165}$ were: 5'-CGAGAC GCAGCGACAAGGCA-3' (forward) and 5'-ACCTTCTCC AAACCGTTGGCA-3' (reverse). Primers for rat hypoxia-inducible factor-1α (HIF-1α) were: 5'-GCCCAGTGAGAA AGGGGAAA-3' (forward) and 5'-CGGCTGGTTACTGCT GGTAT-3' (reverse). Primers for rat glyceraldehyde 3-phosphate dehydrogenase (GAPDH) were: 5'-TGATGGGTGTGA ACCACGAG-3' (forward) and 5'-CCCTTCCACGATGCC AAAGT-3' (reverse). Real-time PCR was performed according to the methods described previously (15).

Enzyme-linked immunosorbent assay (ELISA). Before rats were sacrificed, blood samples were drawn from the inferior caval vein. The samples were immediately centrifuged over 10 min at 3,000 rpm. The supernatant fluid was stored in a refrigerator at -40˚C for further analysis. $VEGF_{165}$ and HIF-1α serum levels were detected by the ELISA assay kit (USCN Life Science Inc., Wuhan, China).

Immunohistochemistry. Immunohistochemical analysis was performed as previously described (16). In brief, deparaffinized tissue sections (4-μm) were blocked with 10% goat serum for 30 min at 37˚C. Primary antibodies against CD31 (1:500 rabbit anti-rat CD31) and $VEGF_{165}$ (1:250 rabbit anti-rat VEGF) (both from Abcam, Cambridge, MA, USA) were used. After primary antibody incubation, the sections reacted with a secondary antibody (1:1,000 goat anti-rat; Abcam). All the sections were counterstained with hematoxylin. Immunoreactivity for CD31 and VEGF were calculated using the Image-Pro Plus 4.0 analysis system software (Media Cybernetics, Inc.). Capillaries were defined by positive staining for CD31. Results were expressed based on the average number of capillaries per 10x field (17).

Western blotting. Western blot analysis was performed as previously described (18). In brief, proteins from myocardium tissues and HUVECs were extracted by homogenization in a lysis buffer containing protease inhibitors and separated by sodium dodecyl sulfate-polyacrylamide gel electrophoresis. Proteins were then transferred to a polyvinylidene fluoride (PVDF) membrane (Roche Applied Science, Penzberg, Germany). After incubation in 5% non-fat milk, the membranes were incubated with primary antibodies against PKCβ2 (1:500), p-PKCβ2 (Thr^{641}) (1:250), Akt (1:1,000), p-Akt (Ser^{473}) (1:500), eNOS (1:1,000), p-eNOS (Ser^{1117}) (1:500), $VEGF_{165}$ (1:250) and HIF-1α (1:500) (all from Abcam), overnight at 4˚C. Membranes were washed three times with 1‰ Tris-buffered saline and Tween-20 (TBST) and incubated with a secondary antibody for 1.5 h at room temperature. After washing three times, proteins were detected by the ECL system (Roche Applied Science). Bands were quantified by densitometry using the Image J software (version 1.41; National Institutes of Health, Bethesda, MD, USA).

Statistical analysis. Data are expressed as means ± SD. All data analyses were performed with SPSS 13.0 statistical software (SPSS Inc., Chicago, IL, USA). Non-parametric data concerning survival rate were analyzed using the Chi-square test or Fisher's exact method. One-way ANOVA followed by the Student-Newman-Keuls test was used to compare the effect of treatment on the various parameters. $P<0.05$ was considered to indicate a statistically significant difference.

Results

Effect of LY333 on the H-G-induced decrease of tube formation by HUVECs. To determine whether LY333 decreased the ability of HUVECs to form capillary-like tubes by H-G (33.3 mmol/l), HUVECs cultured in L-G (5.6 mmol/l) and HUVECs exposed to H-G in the presence or absence of LY333 (10 nmol/l) were seeded at $1x10^4$/well and the tube formation was detected microscopically. After 18 h of culturing, the capacity for tube formation of HUVECs on Matrigel was significantly reduced in the H-G group compared to the L-G group (Fig. 1A and B), whereas LY333 significantly improved its ability for tube formation of HUVECs in H-G medium (Fig. 1C).

Effect of LY333 on the decrease of HUVECs migration and proliferation induced by H-G. To assess the effect of LY333 on HUVECs migration using a wound healing assay, wounds were produced by scraping cells with a 200 μl pipette tip (Fig. 2A). Cells were cultured with different concentrations of glucose for 24 h. Wounds were observed with a microscope at x40 (Fig. 2A). Incubation of cells in H-G (33.3 mmol/l) medium significantly decreased the migratory capacity compared to the L-G (5.6 mmol/l) group (30±5.3 vs. 50±6.1%, $P<0.05$), whereas LY333 significantly prevented the H-G-induced decrease of HUVECs migration (48±4.9 vs. 30±5.3%, $P<0.05$) (Fig. 2B). Taken together, these results indicate that LY33351 improves endothelial cell migration in H-G environment.

HUVECs proliferation in different conditions was assessed by MTT assay. After seeding, HUVECS were cultured in different conditions for 24 h. Incubation of HUVECs with H-G medium significantly reduced their proliferation compared with the L-G medium (55±5.8 vs. 128±10.1%, $P<0.01$) (Fig. 2C). Compared with the H-G group, HUVECs treated with LY333 showed a higher rate of proliferation in H-G medium (115±7.6 vs. 55±5.8%, $P<0.01$) (Fig. 2C). These results suggest that LY333 improves HUVECs proliferation incubated in H-G medium.

Effect of LY333 on p-PKCβ2, p-Akt and p-eNOS expression in HUVECs. We determined whether PKCβ2 activation was induced by H-G levels and if there was any effect on phosphorylation of Akt and eNOS in HUVECs. H-G HUVECs, but not L-G, had a significantly increased PKCβ2 activation after 24 h (Fig. 3B) and a decreased phosphorylation of Akt and eNOS (Fig. 3C and D). Treatment of HUVECs with LY333 not only reduced H-G-induced PKCβ2 activation (Fig. 3B), but also prevented the decrease in phosphorylation of Akt and eNOS (Fig. 3C and D). These data indicated that the activation of PKCβ2 induced by H-G may decrease phosphorylation of Akt and eNOS.

LY333 improved cardiac geometry, performance and hemodynamics. Four weeks after MI the cardiac geometry and performance were evaluated by echocardiography (Table I). In the MI group, significantly decreased LVEF and FS with

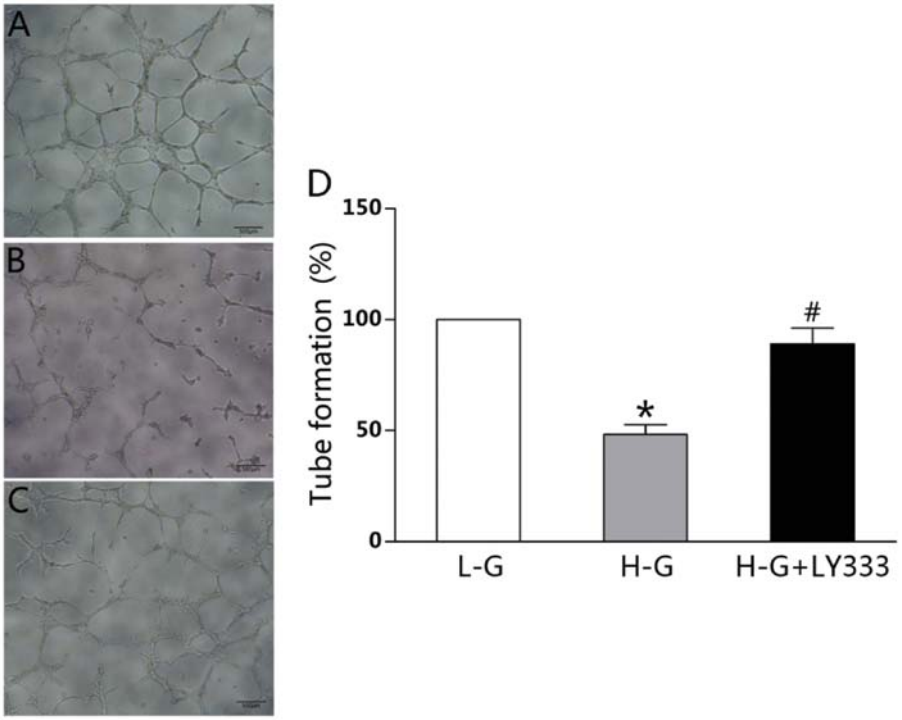

Figure 1. Effect of LY333531 (LY333) on high glucose (H-G)-induced human umbilical vein endothelial cells (HUVECs) tube formation reduction. Tube formation in the (A) low glucose (L-G) (5.6 mmol/l, glucose), (B) H-G group (33.3 mmol/l, glucose) and (C) H-G + LY333 group (10 μmol/l, LY333), scale bar, 500 μm. (D) H-G significantly reduced HUVECs tube formation. Co-incubation with LY333, a specific PKCβ2 inhibitor, markedly improved tube formation. (n=3, mean ± SD). *P<0.05 vs. L-G group; $^{\#}$P<0.05 vs. H-G group.

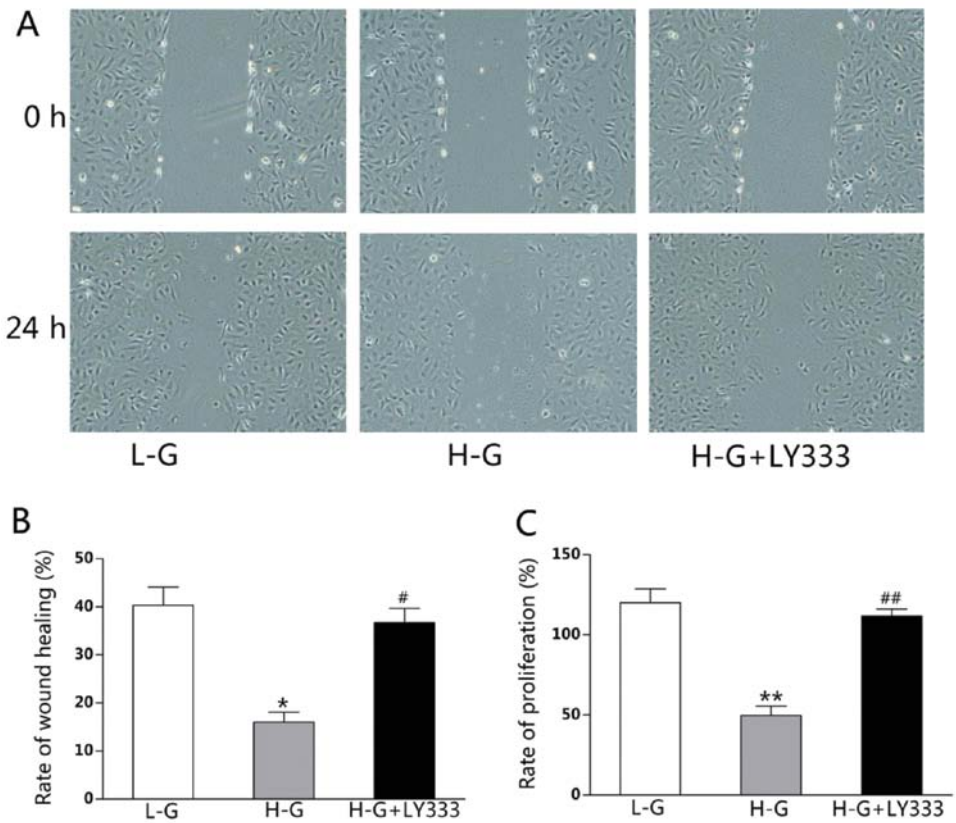

Figure 2. LY333531 (LY333) improved the high glucose (H-G)-induced decrease of human umbilical vein endothelial cell (HUVECs) migration and proliferation. (A and B) Wound healing assay performed to evaluate the migration of HUVECs in different conditions. (C) 3-(4,5-dimethylthiazol-2-yl)-2,5-diphenyltetrazolium bromide (MTT) assay was used to determine the proliferation of HUVECs. Data are expressed as means ± SD (n=3 in each group). *P<0.05 and **P<0.01 vs. glucose (L-G) group; $^{\#}$P<0.05 and $^{\#\#}$P<0.01 vs. H-G group.

Table I. Cardiac geometry, performance and hemodynamic parameters.

Parameters	Sham	MI	LY333
No.	10	14	14
Survival	10	11	12
LVESd (mm)	3.70±0.30	6.0±0.21[a]	4.4±0.19[a,b]
LVEDd (mm)	6.72±0.19	8.69±0.23[a]	7.5±0.29[a,b]
LVEF (%)	85.6±5.42	49.3±6.92[a]	66.8±7.21[a,b]
FS (%)	78.8±4.32	45.8±2.89[a]	67.3±5.21[a,b]
LVEDP (mmHg)	7.9±0.98	14.5±1.43[a]	11.3±1.01[a,b]
+dp/dt$_{max}$ (mmHg/s)	6421±299	4637±253[a]	5721±275[a,b]
-dp/dt$_{max}$ (mmHg/s)	5267±335	3487±301[a]	4894±278[a,b]
Heart rate (bpm)	325±6	341±10	336±8

Echocardiographic and hemodynamic parameters were obtained 4 weeks after operation. Results are expressed as means ± SD. [a]P<0.05 vs. sham-operated group; [b]P<0.05 vs. MI group. LVESd, left ventricular end-systolic; LVEDd, left ventricular end-diastolic diameters; LVEF, left ventricular ejection fraction; FS, fractional shortening; LVEDP, left ventricular end-diastolic pressure.

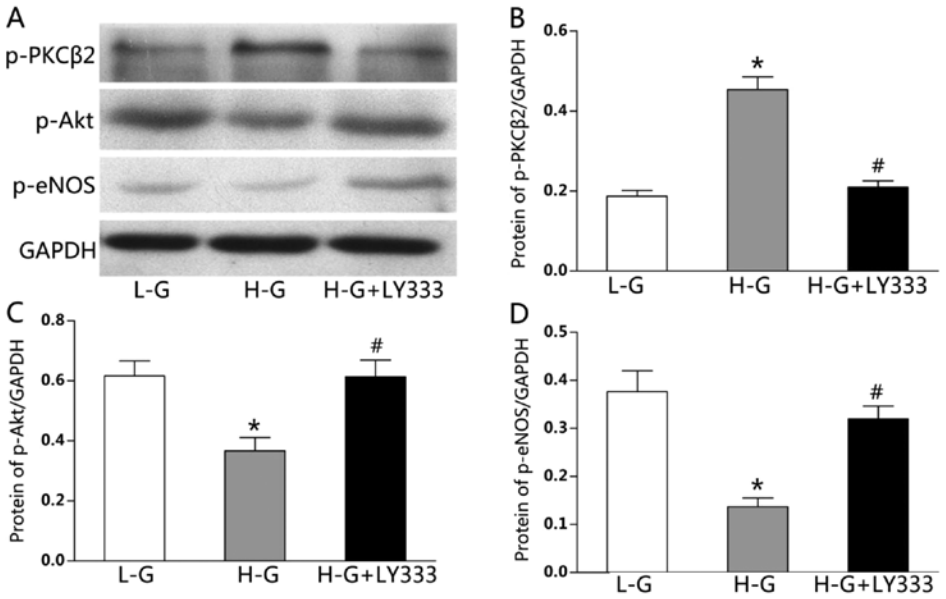

Figure 3. Effect of LY333531 (LY333) on the expression of PKCβ2, Akt and endothelial nitric oxide synthase (eNOS) phosphorylation in human umbilical vein endothelial cells (HUVECs). (A) Representative western blot results for p-PKCβ2, p-Akt, and p-eNOS. (B-D) Quantitative assessment of the expression of PKCβ2, Akt and eNOS phosphorylation, respectively. Data are expressed as means ± SD (n=3). *P<0.05 vs. low glucose (L-G) group; #P<0.05 vs. high glucose (H-G) + LY333 group.

dilated LVESd and LVEDd were observed compared with the sham-operated group (P<0.05, respectively) (Table I). LVESd and LVEDd were significantly reduced in LY333-treated MI rats (P<0.05, vs. MI group, respectively). However, LY333-treated MI rats still exhibited decreased LVEF and FS, increased LVESd and LVEDd compared with the sham-operated rats (P<0.05, respectively). Being consistent with improved echocardiographic parameters, LY333-treated MI rats increased the left ventricular positive and negative dP/dT$_{max}$, and decreased the LVEDP (P<0.05, vs. MI group, respectively) (Table I). Although MI rats treated with LY333 had an increased survival rate compared to MI rats, statistical significance was not achieved (86 vs. 79%, P>0.05) (Table I). There were no significant differences among groups in terms of HR.

LY333 reduced myocardial infarct size. To evaluate the effect of LY333 on infarct size, the latter was quantified in all 3 groups 4 weeks after MI (Fig. 4). There was reduction of the infarct size in the LY333-treated group compared to the MI group (26.7±2.7 vs. 46.3±4.1%, P<0.05).

LY333 increased myocardium capillary density after MI. To assess the effect of LY333 on VEGF expression and myocardium capillary density, immunohistochemical staining for VEGF was performed and showed that myocardium VEGF expression levels were increased in the MI and LY333 groups, compared with the sham-operated group (P<0.05) (Fig. 5A, B and D). Although immunohistochemical staining for CD31 revealed that the density of CD31-positive

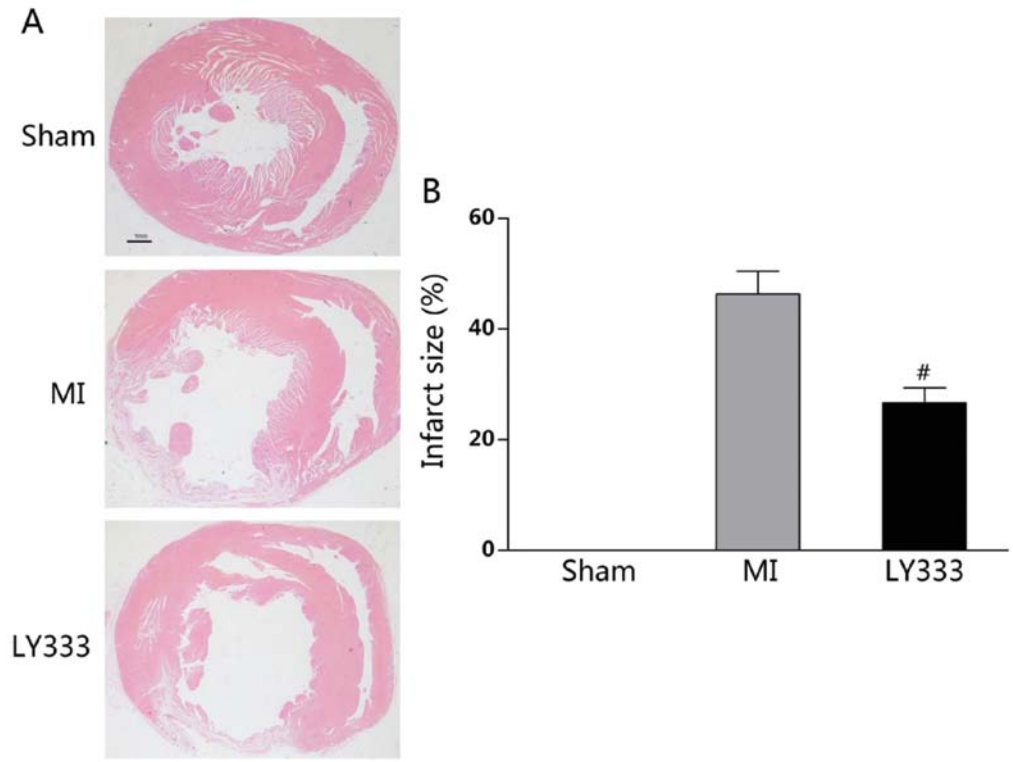

Figure 4. Effect of LY333531 (LY333) on myocardial infarct size. Representative Masson's trichrome-stained LV sections obtained 4 weeks after myocardial infarction (MI) from each group. Scale bar, 100 mm. (A) The necrotic area and viable myocardium are identified in white and red, respectively. (B) Quantitative assessment of infarct size. Data are expressed as means ± SD (n=8-10). $^{\#}$P<0.05 vs. MI group.

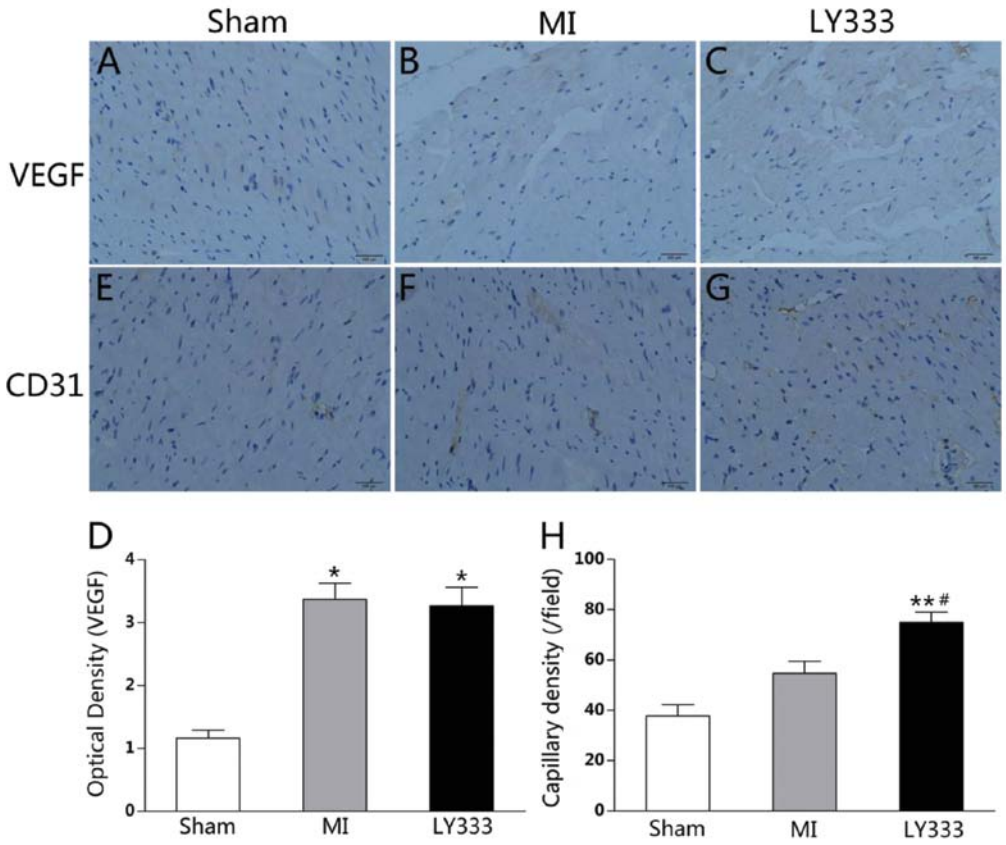

Figure 5. Effect of LY333531 (LY333) on myocardial vascular endothelial growth factor (VEGF) and CD31 expression in diabetic rats. (A-C and E-G) Immunohistochemical staining for VEGF and CD31 were performed in each group 4 weeks after operation. Scale bar, 100 μm. (D) Quantitative assessment of VEGF expression in the myocardium of diabetic rats. (H) Quantitative assessment of capillary density in the myocardium, assessed by CD31 expression in each group. Data are expressed as means ± SD (n=8-10). *P<0.05 and **P<0.01 vs. sham-operated group; $^{\#}$P<0.05 vs. myocardial infarction (MI) group.

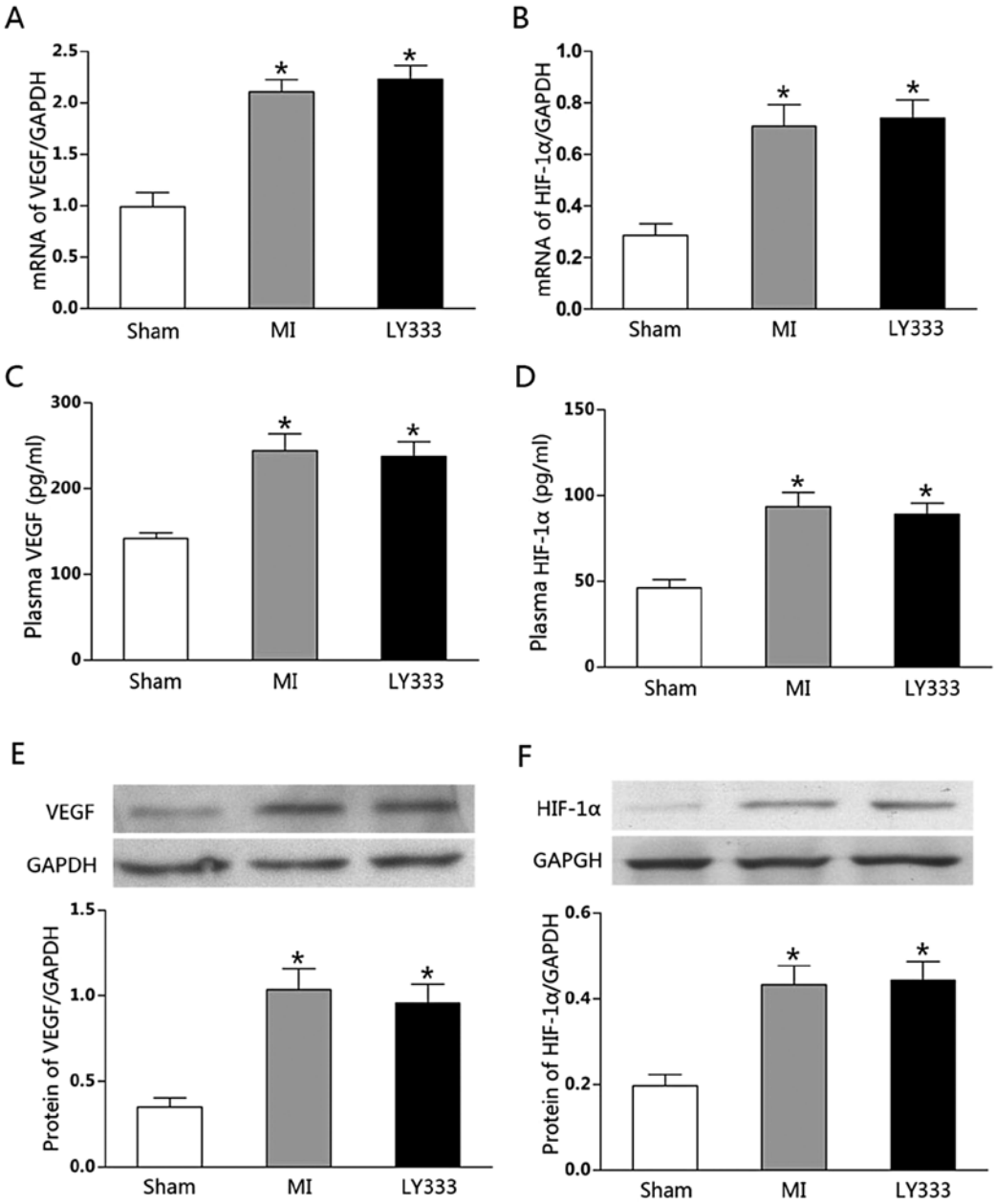

Figure 6. Effect of LY333531 (LY333) on vascular endothelial growth factor (VEGF) and hypoxia-inducible factor-1α (HIF-1α) expression at the mRNA and protein levels, and in serum levels. (A and B) VEGF and HIF-1α expression in myocardium were quantified for their (C and D) mRNA and protein expression, and their (E and F) protein expression levels in plasma measured by ELISA. Data are expressed as means ± SD (n=8-10). *P<0.05 vs. sham-operated group.

microvessels was increased in MI rats compared with the sham-operated rats (Fig. 5E and F), it did not reach statistical significance (P>0.05) (Fig. 5H). Although there was no significant difference between the MI and LY333 groups for myocardium VEGF expression (P>0.05) (Fig. 5D), LY333 administration, after MI, significantly increased the density of CD31-positive blood vessels compared to the remaining groups (P<0.01, vs. sham-operated group; P<0.05, vs. MI group) (Fig. 5E-H).

LY333 did not significantly increase VEGF and HIF-1α expression at the mRNA and protein levels, and in plasma levels. LY333 treatment did not result in significant increases in VEGF and HIF-1α expression at the mRNA and protein levels. Quantitative PCR (qPCR) and western blot analysis demonstrated that MI rats exhibited increases in VEGF and HIF-1α expression at the mRNA (VEGF, 2.1±0.13-fold increase; HIF-1α, 2.5±0.14-fold increase) and protein (VEGF, 2.9±0.14-fold increase; HIF-1α, 2.3±0.12-fold increase) levels in MI rats compared to sham-operated rats (P<0.05, respectively, Fig. 6A-D). However, significant increases in VEGF and HIF-1α expression at the mRNA and protein levels were not detected in the LY333 rat group compared to MI rats without therapy (P>0.05, respectively).

In line with the mRNA and protein expression, MI rats exhibited significant increases in protein expression of VEGF (224±19 pg/ml) and HIF-1α (94±8.1 pg/ml) in plasma, measured by ELISA assay compared to the sham-operated rats (VEGF, 141±7.3 pg/ml; HIF-1α, 46±4.7 pg/ml; P<0.05, respectively) (Fig. 6E and F). Again, however, the VEGF and

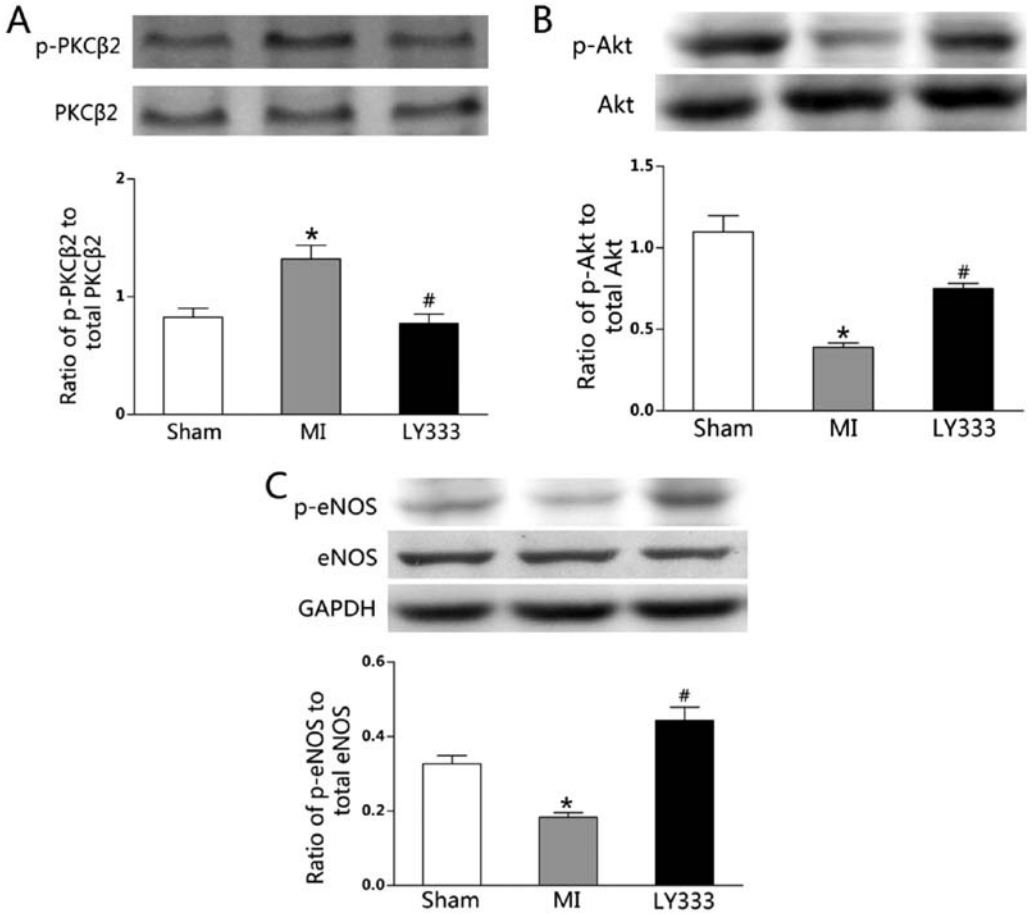

Figure 7. Effect of LY333531 (LY333) on the protein expression of p-PKCβ2, p-Akt and phospho-endothelial nitric oxide synthase (p-eNOS) in myocardium. (A) Representative western blot showing the protein expression of p-PKCβ2, (B) p-Akt and (C) p-eNOS. Data are expressed as mean ± SD (n=8-10). *P<0.05 vs. sham-operated group; #P<0.05 vs. myocardial infarction (MI) group.

HIF-1α protein expression levels in plasma were not significantly increased in LY333-treated rats compared to MI rats without therapy (VEGF, 237±18 pg/ml; HIF-1α, 89±6.7 pg/ml; P>0.05, respectively, vs. MI group).

LY333 increased the expression of p-Akt and p-eNOS in the myocardium. Four weeks after MI, MI rats had a significantly increased myocardium PKCβ2 activation without a significantly decreased Akt and eNOS phosphorylation, compared to the sham-operated rats (Fig. 7). Similar to results observed in HUVECs, LY333-treated MI rats had a significantly reduced PKCβ2 activation (Fig. 7A), and increased Akt and eNOS phosphorylation, compared to the MI group (Fig. 7B and C).

Discussion

In the present study, we observed that LY333, a selective PKCβ2 inhibitor, prevented the *in vitro* decreased tube formation, proliferation and migration observed in HUVECs submitted to H-G levels, partly by increasing Akt and eNOS phosphorylation. Furthermore, using an *in vivo* diabetic rat MI model, we observed that treatment of rats with LY333 significantly improved post-MI cardiac function, and increased the density of the capillaries, as proven by CD31-positive staining in ischemic myocardium. We also demonstrated that LY333 treatment not only inhibits activation of PKCβ2, but also increases the levels of p-Akt and p-eNOS expression in diabetic myocardium. Thus, to the best of our knowledge, the present study has demonstrated for the first time that improved cardiac function after MI by LY333 therapy is partly associated with increased angiogenesis of the ischemic myocardium, which is attributed to inhibition of the PKCβ2-mediated downregulation of the VEGF-dependent Akt/eNOS pathway.

Angiogenesis is the process of sprouting new capillaries from pre-existing blood vessels and plays an important role in pathological and physiological conditions (19). In ischemic diseases, particularly in MI, the post-MI formation of new collateral coronary arteries is important in the recovery of cardiac function. However, the development of collateral coronary arteries in response to MI has been shown to be impaired by hyperglycemia in diabetes, leading to profound ventricular remodeling and subsequent heart failure (20,21). Furthermore, the impairment of myocardial angiogenesis in diabetes has been associated with a decreased VEGF expression or downregulation of VEGF-dependent signaling pathways (22). Therefore, increase of the formation of collateral coronary arteries in diabetic myocardium is expected to improve the cardiac function after MI.

Previous studies have demonstrated that H-G levels increase diacylglycerol (DAG) synthesis, which is a potent activator of PKC isoforms in many cell types (23,24). In H-G condi-

tions, DAG levels are elevated in vascular tissues, such as the aorta, heart, and retina, along with a preferential activation of PKCβ2, one of the classical PKC isoforms (6,25). Furthermore, activation of PKCβ2-mediated transduction pathways may contribute to the pathogenesis of various diabetic vascular complications. Previously, it has been shown that increased angiogenesis, induced by H-G levels, contributes to proliferative vasculopathies, such as diabetic retinopathy and diabetic nephropathy, and that inhibition of PKCβ2 prevents these diabetic complications (26). It is now established that PKCβ2 activation, induced by H-G levels, is crucial in defective angiogenesis in diabetes, such as impaired wound healing (27) and embryonic growth (28). Moreover, recent studies have demonstrated that the inhibition of PKCβ2 prevented post-MI cardiac dysfunction and that it was associated with reduction of cardiac interstitial fibrosis and inflammation (8,9). However, few studies are available reporting the effect of PKCβ2 inhibition on hyperglycemia-induced impaired myocardium angiogenesis after MI.

In the present study, in an *in vitro* setting, we tested the hypothesis that H-G-induced activation of PKCβ2 decreased the VEGF-dependent Akt/eNOS pathway, leading to decreased tube formation, proliferation and migration of HUVECs. Notably, our results provide clear evidence supporting this hypothesis because treatment with LY333 restored tube formation, proliferation, and migration abilities of HUVECs submitted to H-G levels. In addition, LY333 treatment prevented the activation of PKCβ2 and increased the levels of p-Akt and p-eNOS expression in HUVECs exposed to H-G, indicating that H-G induces activation of PKCβ2 to mediate downregulation of Akt/eNOS pathway. *In vivo*, using a model of diabetic MI rats, we have shown that LY333 treatment not only prevents the post-MI deterioration of cardiac function, but also significantly reduces infarct size, confirming the hypothesis that PKCβ2 inhibition improves post-MI cardiac function. Of note, we observed that rats treated with LY333 present a significant increase in the density of capillaries in the ischemic myocardium compared to rats without therapy. This increase in vascularization may be responsible for the significant reduction in the myocardial fibrosis and marked increase in viable cardiac tissue in the infarct and peri-infarct regions of the diabetic myocardium. Therefore, supporting improved cardiac function post-MI, by PKCβ inhibition, may attribute to increased angiogenesis in diabetic ischemic myocardium. However, it has also been shown that activation of PKCβ post-MI induces an increase of fibrosis and pro-inflammatory responses (8,9). In the present study we cannot exclude the possibility that improved cardiac function post-MI, by PKCβ inhibition, may contribute to the reduction of fibrosis and inflammation.

VEGF expression affected by ischemia has been shown to be decreased in diabetic myocardiums. In addition, downregulation of VEGF expression may provide a possible explanation for the impaired formation of collateral coronary capillaries in an ischemic myocardium (29,30). In the diabetic MI animals, Samuel *et al* (5) demonstrated that intramyocardial administration of adenoviral vectors, encoding VEGF, induces angiogenesis of the ischemic myocardium, thereby improving post-MI cardiac function, confirming the hypothesis that impairment of angiogenesis is associated with a decrease in the VEGF expression of the diabetic myocardium. However, the present study showed that LY333 treatment of rats significantly increased angiogenesis of the ischemic myocardium, which may eventually improve post-MI cardiac function compared with rats without therapy. Apart from the increased capillary density there was also a significant increase of VEGF expression at the mRNA and protein levels in the ischemic myocardium, indicating that increased angiogenesis of ischemic myocardium by LY333 cannot be fully attributed to upregulation of the VEGF expression in ischemic myocardium. However, it has recently been shown that H-G impaired angiogenesis without altering the expression level of VEGF through induction of apoptosis and decreased proliferation of endothelial cells (31), and that hyperglycemia-induced activation of PKCβ2 inhibited the activation of the VEGF dependent-Akt/eNOS pathway (7). In the present study, we confirmed that the H-G-induced activation of PKCβ2 led to a decrease in Akt and eNOS phosphorylation in HUVECs. In addition, we showed that a significant increase in PKCβ2 activity was observed in the myocardium of MI rats, which can lead to decreased VEGF expression in the myocardium of MI diabetic rats (32). Treatment of HUVECs with LY333 not only prevented PKCβ2 activation, but also attenuated the decreased phosphorylation of Akt and eNOS in H-G conditions. Similar results were observed in HUVECs with the treatment of diabetic rats with LY333 after MI. Significantly attenuated PKCβ2 activation and increased Akt and eNOS phosphorylation were observed in the ischemic myocardium. However, VEGF expression in the myocardium of MI rats was not significantly elevated in the LY333 group compared to the MI group. Thus, our results support that activation of PKCβ2-mediated downregulation of the VEGF-dependent Akt/eNOS pathway may lead to decreased capillary formation in ischemic myocardiums of diabetic MI rats.

In conclusion, to the best of our knowledge, we report for the first time that inhibition of PKCβ2 by LY333 effectively improves cardiac function after MI and that the beneficial effect is closely associated with the increased density of collateral coronary arteries in the ischemic myocardium of diabetic rats, which is due to attenuation of the activation of PKCβ2-mediated downregulation of the VEGF-dependent Akt/eNOS pathway.

References

1. Flaherty JD and Davidson CJ: Diabetes and coronary revascularization. JAMA 293: 1501-1508, 2005.
2. Jaffe AS, Spadaro JJ, Schechtman K, Roberts R, Geltman EM and Sobel BE: Increased congestive heart failure after myocardial infarction of modest extent in patients with diabetes mellitus. Am Heart J 108: 31-37, 1984.
3. Stone PH, Muller JE, Hartwell T, York BJ, Rutherford JD, *et al*: The effect of diabetes mellitus on prognosis and serial left ventricular function after acute myocardial infarction: contribution of both coronary disease and diastolic left ventricular dysfunction to the adverse prognosis. The MILIS Study Group. J Am Coll Cardiol 14: 49-57, 1989.
4. Ishihara M, Inoue I, Kawagoe T, Shimatani Y, Kurisu S, *et al*: Impact of acute hyperglycemia on left ventricular function after reperfusion therapy in patients with a first anterior wall acute myocardial infarction. Am Heart J 146: 674-678, 2003.
5. Samuel SM, Akita Y, Paul D, Thirunavukkarasu M, Zhan L, *et al*: Coadministration of adenoviral vascular endothelial growth factor and angiopoietin-1 enhances vascularization and reduces ventricular remodeling in the infarcted myocardium of type 1 diabetic rats. Diabetes 59: 51-60, 2010.

6. Inoguchi T, Battan R, Handler E, Sportsman JR, Heath W and King GL: Preferential elevation of protein kinase C isoform beta II and diacylglycerol levels in the aorta and heart of diabetic rats: differential reversibility to glycemic control by islet cell transplantation. Proc Natl Acad Sci USA 89: 11059-11063, 1992.
7. Naruse K, Rask-Madsen C, Takahara N, Ha SW, Suzuma K, *et al*: Activation of vascular protein kinase C-beta inhibits Akt-dependent endothelial nitric oxide synthase function in obesity-associated insulin resistance. Diabetes 55: 691-698, 2006.
8. Boyle AJ, Kelly DJ, Zhang Y, Cox AJ, Gow RM, *et al*: Inhibition of protein kinase C reduces left ventricular fibrosis and dysfunction following myocardial infarction. J Mol Cell Cardiol 39: 213-221, 2005.
9. Palaniyandi SS, Ferreira JC, Brum PC and Mochly-Rosen D: PKCβII inhibition attenuates myocardial infarction induced heart failure and is associated with a reduction of fibrosis and pro-inflammatory responses. J Cell Mol Med 15: 1769-1777, 2011.
10. Miura S, Matsuo Y and Saku K: Transactivation of KDR/Flk-1 by the B2 receptor induces tube formation in human coronary endothelial cells. Hypertension 41: 1118-1123, 2003.
11. Leavesley DI, Schwartz MA, Rosenfeld M and Cheresh DA: Integrin beta 1- and beta 3-mediated endothelial cell migration is triggered through distinct signaling mechanisms. J Cell Biol 121: 163-170, 1993.
12. Shi F, Wang YC, Zhao TZ, Zhang S, Du TY, *et al*: Effects of simulated microgravity on human umbilical vein endothelial cell angiogenesis and role of the PI3K-Akt-eNOS signal pathway. PLoS One 7: e40365, 2012.
13. Wei L, Yin Z, Yuan Y, Hwang A, Lee A, *et al*: A PKC-beta inhibitor treatment reverses cardiac microvascular barrier dysfunction in diabetic rats. Microvasc Res 80: 158-165, 2010.
14. Derumeaux G, Mulder P, Richard V, Chagraoui A, Nafeh C, *et al*: Tissue Doppler imaging differentiates physiological from pathological pressure-overload left ventricular hypertrophy in rats. Circulation 105: 1602-1608, 2002.
15. Meng D, Lv DD and Fang J: Insulin-like growth factor-I induces reactive oxygen species production and cell migration through Nox4 and Rac1 in vascular smooth muscle cells. Cardiovasc Res 80: 299-308, 2008.
16. Tang JM, Wang JN, Zhang L, Zheng F, Yang JY, *et al*: VEGF/SDF-1 promotes cardiac stem cell mobilization and myocardial repair in the infarcted heart. Cardiovasc Res 91: 402-411, 2011.
17. Xie J, Lu W, Gu R, Dai Q, Zong B, *et al*: The impairment of ILK related angiogenesis involved in cardiac maladaptation after infarction. PLoS One 6: e24115, 2011.
18. Kelly DJ, Cox AJ, Gow RM, Zhang Y, Kemp BE and Gilbert RE: Platelet-derived growth factor receptor transactivation mediates the trophic effects of angiotensin II in vivo. Hypertension 44: 195-202, 2004.
19. Folkman J: Angiogenesis in cancer, vascular, rheumatoid and other disease. Nat Med 1: 27-31, 1995.
20. Abaci A, Oğuzhan A, Kahraman S, Eryol NK, Unal S, *et al*: Effect of diabetes mellitus on formation of coronary collateral vessels. Circulation 99: 2239-2242, 1999.
21. Martin A, Komada MR and Sane DC: Abnormal angiogenesis in diabetes mellitus. Med Res Rev 23: 117-145, 2003.
22. Chen JX and Stinnett A: Disruption of Ang-1/Tie-2 signaling contributes to the impaired myocardial vascular maturation and angiogenesis in type II diabetic mice. Arterioscler Thromb Vasc Biol 28: 1606-1613. 2008.
23. Lee TS, Saltsman KA, Ohashi H and King GL: Activation of protein kinase C by elevation of glucose concentration: proposal for a mechanism in the development of diabetic vascular complications. Proc Natl Acad Sci USA 86: 5141-5145, 1989.
24. Wolf BA, Williamson JR, Easom RA, Chang K, Sherman WR, *et al*: Diacylglycerol accumulation and microvascular abnormalities induced by elevated glucose levels. J Clin Invest 87: 31-38, 1991.
25. Shiba T, Inoguchi T, Sportsman JR, Heath WF, Bursell S and King GL: Correlation of diacylglycerol level and protein kinase C activity in rat retina to retinal circulation. Am J Physiol 265: 783-793, 1993.
26. Koya D and King GL: Protein kinase C activation and the development of diabetic complications. Diabetes 47: 859-866, 1998.
27. Kämpfer H, Pfeilschifter J and Frank S: Expressional regulation of angiopoietin-1 and -2 and the tie-1 and -2 receptor tyrosine kinases during cutaneous wound healing: a comparative study of normal and impaired repair. Lab Invest 81: 361-373, 2001.
28. Pinter E, Mahooti S, Wang Y, Imhof BA and Madri JA: Hyperglycemia-induced vasculopathy in the murine vitelline vasculature: correlation with PECAM-1/CD31 tyrosine phosphorylation state. Am J Pathol 154: 1367-1379, 1999.
29. Chou E, Suzuma I, Way KJ, Opland D, Clermont AC, *et al*: Decreased cardiac expression of vascular endothelial growth factor and its receptors in insulin-resistant and diabetic States: a possible explanation for impaired collateral formation in cardiac tissue. Circulation 105: 373-379, 2002.
30. Waltenberger J, Lange J and Kranz A: Vascular endothelial growth factor-A-induced chemotaxis of monocytes is attenuated in patients with diabetes mellitus: a potential predictor for the individual capacity to develop collaterals. Circulation 102: 185-190, 2000.
31. Larger E, Marre M, Corvol P and Gasc JM: Hyperglycemia-induced defects in angiogenesis in the chicken chorioallantoic membrane model. Diabetes 53: 752-761, 2004.
32. Ikeda A, Matsushita S and Sakakibara Y: Inhibition of protein kinase C β ameliorates impaired angiogenesis in type I diabetic mice complicating myocardial infarction. Circ J 76: 943-949, 2012.